Evidence for TeV Gamma-Ray Emission from a Region of the Galactic Plane

R. Atkins,[1,*] W. Benbow,[2,†] D. Berley,[3] E. Blaufuss,[3] D. G. Coyne,[2] T. DeYoung,[3] B. L. Dingus,[4] D. E. Dorfan,[2] R. W. Ellsworth,[5] L. Fleysher,[6] R. Fleysher,[6] G. Gisler,[4] M. M. Gonzalez,[1] J. A. Goodman,[3] T. J. Haines,[4] E. Hays,[3] C. M. Hoffman,[4] L. A. Kelley,[2] C. P. Lansdell,[3] J. T. Linnemann,[7] J. E. McEnery,[1,‡] R. S. Miller,[8] A. I. Mincer,[6] M. F. Morales,[2,§] P. Nemethy,[6] D. Noyes,[3] J. M. Ryan,[8] F. W. Samuelson,[4] P. M. Saz Parkinson,[2] A. Shoup,[9] G. Sinnis,[4] A. J. Smith,[3] G. W. Sullivan,[3] D. A. Williams,[2] M. E. Wilson,[1] X. W. Xu,[4] and G. B. Yodh[9]

[1]*Department of Physics, University of Wisconsin, 1150 University Avenue, Madison, Wisconsin 53706, USA*
[2]*Santa Cruz Institute for Particle Physics, University of California, 1156 High Street, Santa Cruz, California 95064, USA*
[3]*Department of Physics, University of Maryland, College Park, Maryland 20742, USA*
[4]*Group P-23, Los Alamos National Laboratory, P.O. Box 1663, Los Alamos, New Mexico 87545, USA*
[5]*Department of Physics and Astronomy, George Mason University, 4400 University Drive, Fairfax, Virginia 22030, USA*
[6]*Department of Physics, New York University, 4 Washington Place, New York, New York 10003, USA*
[7]*Department of Physics and Astronomy, Michigan State University, 3245 BioMedical Physical Sciences Building, East Lansing, Michigan 48824, USA*
[8]*Department of Physics, University of New Hampshire, Morse Hall, Durham, New Hampshire 03824, USA*
[9]*Department of Physics and Astronomy, University of California, Irvine, California 92697, USA*

(Received 15 February 2005; revised manuscript received 5 October 2005; published 16 December 2005)

Gamma-ray emission from a narrow band at the galactic equator has previously been detected up to 30 GeV. We report evidence for a TeV gamma-ray signal from a region of the galactic plane by Milagro, a large-field-of-view water Cherenkov detector for extensive air showers. An excess with a significance of 4.5 standard deviations has been observed from the region of galactic longitude $l \in (40°, 100°)$ and latitude $|b| < 5°$. Under the assumption of a simple power law spectrum, with no cutoff in the EGRET-Milagro energy range, the measured integral flux is $\phi_\gamma(>3.5\ \mathrm{TeV}) = (6.4 \pm 1.4 \pm 2.1) \times 10^{-11}\ \mathrm{cm}^{-2}\,\mathrm{s}^{-1}\,\mathrm{sr}^{-1}$. This flux is consistent with an extrapolation of the EGRET spectrum between 1 and 30 GeV in this galactic region.

DOI: 10.1103/PhysRevLett.95.251103 PACS numbers: 98.35.−a, 95.85.Pw, 96.40.Pq, 98.70.Rz

Gamma rays are the best direct probe of cosmic rays outside the solar neighborhood. The interstellar medium, with its relatively high density in the galactic plane, is a passive target for gamma-ray production by energetic cosmic rays. Mechanisms include interactions with gas cloud nuclei that produce gamma rays via π^0 decay, cosmic-ray electron bremsstrahlung, and inverse Compton scattering with the interstellar radiation field. Emission from a diffuse source concentrated in the narrow band along the galactic equator was, indeed, detected by the space-borne detectors SAS 2, COS B [1], and notably EGRET [2] at energies up to 30 GeV. Above 1 GeV, the EGRET data in the region of the galactic center show a hard spectrum $E^{-\alpha}$ with a differential spectral index $\alpha \approx 2.3$, and a flux enhancement of as much as 60%, compared to models with π^0 production as the sole mechanism [3] using the local cosmic-ray spectrum. Models predicting a galactic flux enhanced by up to an order of magnitude over the π^0 mechanism at very high energies were proposed [4–7]. Upper limits have been set in the TeV range [8–10] and above 180 TeV [11].

The Milagro Gamma Ray Observatory [12,13] is a large-field-of-view telescope designed to detect gamma rays near 1 TeV using water Cherenkov techniques to observe air-shower particles that survive to the ground level. It is located at a latitude of 36° and an altitude of 2630 m in the Jemez Mountains, New Mexico, USA. A 60 m × 80 m × 8 m covered pond, filled with clear water, has a top layer of 450 photomultipliers (PMT), used to reconstruct the shower direction with angular resolution of about 0.75° from the relative PMT timing. A bottom layer of 273 PMT's is used for discrimination between gamma-ray and the dominant hadron-induced air showers. A *compactness* cut described in [13] enriches the fraction of gamma rays in the sample. It rejects about 90% of the hadronic back-

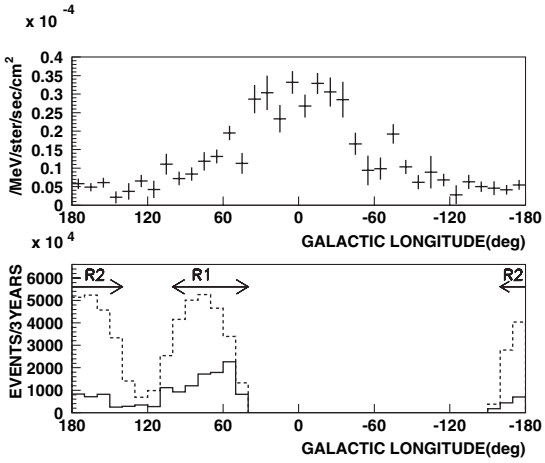

FIG. 1. Top: 4 to 30 GeV EGRET flux. Bottom: Milagro exposure (dashed line) and expected relative significance (solid line), along the galactic equator. Regions *R*1 and *R*2 are indicated.

ground and retains about 45% of the gamma-ray signal for typical gamma-ray source spectra. Reversing this cut produces a gamma-ray-poor sample, used below for a check on systematics. Compared to the compactness-cut signal, the reversed-cut sample contains 9 times more cosmic rays and 1.2 times more gamma rays, so that any gamma signal is suppressed by a factor of 7.4. Additional cuts in this analysis require a minimum of 50 top layer PMT hits, at least 20 of which participate in the angle fit, a zenith angle of $\theta < 50°$, and a declination (DEC) of $10° < \mathrm{DEC} < 60°$. Periods with abnormal event rate, zenith or azimuth distribution, corrupted records, or unstable operation were excluded. The results presented are from three calendar years of data collected by the Milagro detector starting July 2000.

Figure 1 shows the EGRET gamma-ray flux along the galactic equator [2,14] peaking near the galactic center, and the Milagro exposure. The galactic center is not visible to Milagro. Superposed is the nominal expected relative significance, the product of the EGRET flux and the square root of the Milagro exposure. The region $R1$ $[l \in (40°, 100°)]$ with highest expected significance and a second region $R2$ $[l \in (140°, 200°)]$ of high Milagro exposure, both with $|b| < 5°$ were selected *a priori,* as two critical regions for separate statistical tests of a TeV gamma-ray signal. The latitude band size was chosen because it maximizes the statistical sensitivity for a signal that has the EGRET transverse profile. In longitude, the choice was governed by the limits of the Milagro exposure (Fig. 1) and the fact that in the $(100°, 140°)$ longitude region the galactic equator runs parallel to the right ascension (RA) axis, making this region unfavorable for the background estimation method described below. The Milagro exposures in $R1$ and $R2$ are similar. The average

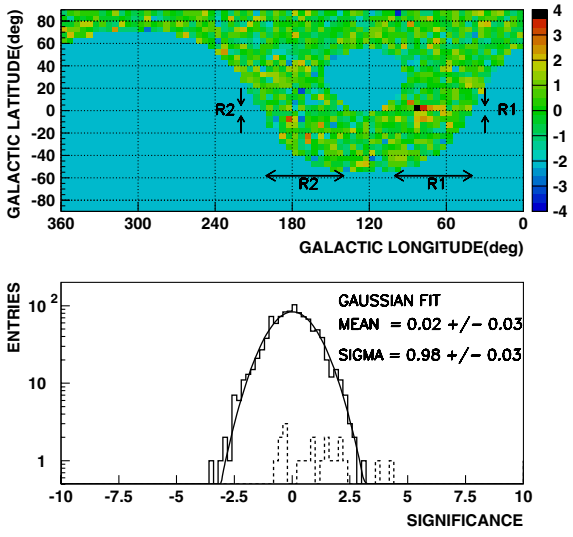

FIG. 2 (color online). Top: Map with a color scale of the significance in galactic coordinates in $5° \times 5°$ bins. Bottom: Significance distribution outside $R1$ (solid line) and inside $R1$ (dashed line).

EGRET flux in $R2$ is about a factor of 2 lower than in $R1$ and the extrapolation to TeV energies may well be different in $R1$ and $R2$. $R1$ includes the cygnus arm and $R2$ is in the extreme outer galaxy.

Gamma-ray emission from a gamma-ray source should appear as an excess of the observed events (N_s) above the expected background count (N_b) in a candidate source direction bin. If the background is isotropic in the celestial coordinate RA and the detector acceptance is not changing over some time window, the number of detected background events can be factorized into a time-independent acceptance shape $G(x)$ in local angular coordinates x (e.g., hour angle and declination) and a time-varying rate $R(t)$. For a candidate source bin of interest ($R1$, $R2$, or any bin of Fig. 2) this gives $N_b = \int_{\text{source bin}} G(x)R(t)dxdt$. We take advantage of a "time-swapping" method [15] to perform a Monte Carlo calculation of this integral. The data are split into 8-hour segments in which the x and t of recorded events are considered random samples of $G(x)$ and $R(t)$. By pairing x and t randomly selected from these samples, new galactic coordinates are generated for background events. N_b is incremented whenever such an event falls into the source bin.

We use a self-consistent modification, described in [16], of the method outlined above. The assumption that $G(x)$ is time independent is relaxed, allowing the incorporation of a small diurnal modulation, from atmospheric changes, that is observed in the zenith distribution of events. The statistical error of the background is calculated with $\sigma^2_{N_b} = AN_b + N_b/B$, where A is the mean on-source to off-source ratio and $B = 10$ is the number of time swaps per event [17]. The events arriving from the galactic plane are excluded from the "time swapping," in order to maintain the statistical independence of N_s and N_b [19].

A very small anisotropy of the cosmic-ray background, at the level of a few parts in 10^4, was observed in a separate Milagro study [21] and is applied as a correction in this analysis. The anisotropy is consistent in shape and magnitude with reports from several other experiments [22–24]. Milagro's observed anisotropy is described adequately by the three longest wavelength harmonics in RA, whose amplitude and phase vary linearly with DEC. The anisotropy study provides a functional form for the background correction in this analysis. The subtracted sky map in RA

TABLE I. Calculation of the fractional excess $\mathcal{F} = (N_s - N_b)/N_b$ for $R1$ and $R2$. N_s is the observed event count; the error is on the mean of the underlying Poisson distribution.

Region	$R1$	$R2$
N_s	$238\,095\,657 \pm 15\,430$	$254\,800\,416 \pm 15\,962$
N_b	$238\,025\,840 \pm 8003$	$254\,826\,272 \pm 8841$
$N_s - N_b$	$69\,817 \pm 17\,382$	$-25\,853 \pm 18\,247$
$\mathcal{F}_{\text{raw}}$	$(2.93 \pm 0.73) \times 10^{-4}$	$(-1.01 \pm 0.72) \times 10^{-4}$
δ_{bg}	$(-0.63 \pm 0.30) \times 10^{-4}$	$(+0.04 \pm 0.30) \times 10^{-4}$
$\mathcal{F}$	$(3.56 \pm 0.79) \times 10^{-4}$	$(-1.05 \pm 0.78) \times 10^{-4}$

DEC coordinates, with $R1$ and $R2$ excluded, is fit to this form, then extrapolated into these regions. The resulting fractional correction of the background, applied in Table I, is $\delta_{\rm bg} = -0.63 \pm 0.30 \times 10^{-4}$ and $\delta_{\rm bg} = +0.04 \pm 0.30 \times 10^{-4}$ for $R1$ and $R2$, respectively; the errors are the statistical errors of the performed fit.

The test for a source signal is done, taking $R1$ and $R2$ as two separate single bins. The steps are given in Table I, with the fractional excess defined by $\mathcal{F} = (N_s - N_b)/N_b$. The statistical errors on $\mathcal{F}$ and $\delta_{\rm bg}$ are combined in quadrature in the last line. An excess with a significance of 4.5 standard deviations is seen in $R1$, while no excess is detected in $R2$.

Figure 2 (top) shows the two-dimensional color map of the significance in galactic coordinates. An enhancement in a ridge along the galactic equator in $R1$ is the most prominent feature. A Gaussian fit to the distribution of significances in Fig. 2 (bottom) has the requisite normal distribution with zero mean and unit variance, while entries from R1 are shifted to the right. Profiles of the fractional excess $\mathcal{F}$ in latitude and longitude are shown in Fig. 3.

To test for possible systematic problems in the analysis of the $R1$ excess, an identical analysis, including all modifications and corrections, was performed on 14 months of data, with the compactness cut reversed to impoverish gamma rays relative to the cosmic-ray background. The result for $R1$, $\mathcal{F}' = (0.68 \pm 0.39) \times 10^{-4}$ agrees well with $\mathcal{F}_{\rm suppressed} = \mathcal{F}/7.4 = (0.48 \pm 0.11) \times 10^{-4}$, which is expected in the absence of systematic effects.

We interpret the excess in $R1$ (Table I) as any combination of diffuse gamma-ray emission, or emission from unresolved point sources or an extended gamma-ray source. The two bins with maximum excess in the longitude profile of Fig. 3 are in the cygnus region, (75°–85°) [25], long known as the location for a peak in the column density for both molecular and atomic hydrogen clouds, inferred from radio emission, and also a pronounced maximum in the EGRET longitude profile in all energy bands [2,26,27]. The ratio of integral gamma-ray to cosmic-ray flux is calculated as

$$\mathcal{R} = \frac{\phi_\gamma}{\phi_{\rm (H+He)}} = \frac{\mathcal{F}}{\eta(\alpha_\gamma)}. \quad (1)$$

Because the intrinsic energy resolution of the Milagro detector is limited, individual event energies were not used in this analysis [28]. The flux determination assumes that the gamma rays have a power law spectrum with no cutoff. The energy scale is determined from air-shower and detector simulations and confirmed by measurements of the Crab Nebula [13]. This gives a median energy of approximately 3.5 TeV, with a 20% systematic error, for gamma rays from the galactic equator. The coefficient $\eta(\alpha_\gamma)$ is the energy and transit averaged ratio of gamma-ray to cosmic-ray effective area, with the compactness cut, obtained with Monte Carlo air-shower and detector simulations [29]. We report results for the power law index connecting the top EGRET point (10–30 GeV) and the Milagro point at 3.5 TeV, $\alpha_\gamma = 2.61$, for which $\eta = 6.2 \pm 2.0$. The error on η is the estimate of Monte Carlo uncertainties, including the energy scale error. We note that the flux is only sensitive to the absolute energy scale of the Milagro in proportion to the difference of power law indices $E^{-(\alpha_\gamma - \alpha_{\rm cr})}$. The cosmic-ray integral flux above 3.5 TeV/nucleus is $\phi_{\rm H+He} = 1.2 \times 10^{-6}$ cm^{-2} s^{-1} sr^{-1} [30]. Integral flux results are shown in Table II and plotted in Fig. 4 together with the EGRET data.

For comparison, we fit the high end (1 to 30 GeV) of the EGRET spectrum [2,14] in $R1$ to a power law, obtaining the index $\alpha_{\gamma\rm (EGRET)} = 2.51 \pm 0.05$, softer than the galactic center value of $\alpha \approx 2.3$, quoted earlier. Extrapolations of the EGRET fits in $R1$ and $R2$, with their 1 standard deviation error corridors, are superposed on Fig. 4.

As seen in Fig. 4, the emission from $R1$ at a 3.5 TeV median energy is consistent with the extrapolation from the high-end EGRET data between 1 and 30 GeV. The absence of a detected excess in $R2$ requires a steepening of the power law to $\alpha_\gamma(R2) > 2.66$ (99% C.L.) compared to

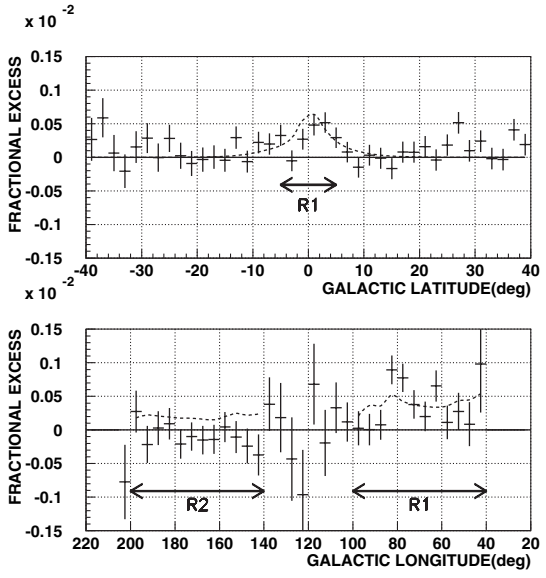

FIG. 3. Profiles of the fractional excess in latitude for the $R1$ longitude band $l \in (40°, 100°)$, and in longitude for the latitude band $|b| < 5°$ of $R1$ and $R2$. The dashed lines show the EGRET source shape.

TABLE II. Ratio of the Milagro gamma-ray to cosmic-ray flux, integral flux above 3.5 TeV (in cm^{-2}s^{-1}sr^{-1}), and the connecting EGRET-Milagro power law index, for region $R1$. The last column uses a fit of the longitude profile in Fig. 3 (bottom) to the EGRET source shape. The results are not sensitive to this choice.

	Single bin	Multibin fit
$\mathcal{R}$	$(5.7 \pm 1.3 \pm 1.8) \times 10^{-5}$	$(6.1 \pm 1.3 \pm 1.9) \times 10^{-5}$
ϕ_γ	$(6.8 \pm 1.5 \pm 2.2) \times 10^{-11}$	$(7.3 \pm 1.5 \pm 2.3) \times 10^{-11}$
α_γ	$2.61 \pm 0.03 \pm 0.05$	$2.60 \pm 0.03 \pm 0.05$

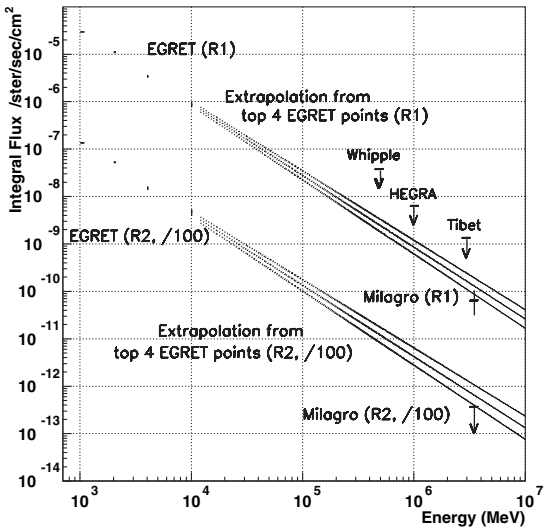

FIG. 4. Integral flux results of Milagro and EGRET detectors, with 99% C.L. upper limits from Whipple [$l \in (38.5°, 41.5°)$, $|b| < 2°$] [8], HEGRA [$l \in (38°, 43°)$, $|b| < 5°$] [9], Tibet [$l \in (20°, 55°)$, $|b| < 5°$] [10]. The display for region $R2$ is shifted by 10^{-2}.

$\alpha_\gamma(R1) = 2.61 \pm 0.03$. The Milagro flux upper limit of $\phi_\gamma(>3.5\ \mathrm{TeV}) < 4 \times 10^{-11}\ \mathrm{cm}^{-2}\,\mathrm{s}^{-1}\,\mathrm{sr}^{-1}$ (99° C.L.) in $R2$ touches the EGRET corridor for that region.

These findings do not require models predicting a strong enhancement of the diffuse flux compared to conventional mechanisms, such as an increased inverse Compton component [31], a harder proton spectrum in the galactic plane [6], or contributions from unresolved supernova remnants [5]. Assuming a power law spectrum for gamma rays with no cutoff below 10 TeV, we can exclude for $R1$ a hard spectrum with power law index $\alpha_\gamma < 2.48$ (99% C.L.). The results are consistent with a gamma-ray power law index that asymptotically approaches that of cosmic rays, as predicted if π^0 production becomes the main source of the gamma flux [3].

In summary, the Milagro detector has observed a 4.5 standard deviation excess in the midlongitude galactic plane region $R1$. The consistency of EGRET and Milagro data under the simple power law assumption reduces the motivation for speculation about more complicated gamma-ray spectra. With its one integral measurement, however, the Milagro finding cannot rule out alternate models. For the many possible multiparameter models the Milagro result provides one constraint in their parameter space. For a simple continuous power law spectrum from EGRET to Milagro energies, this measurement is evidence for gamma-ray emission at TeV energies, with a flux that is consistent with an extrapolation from EGRET, and a median energy of about 3.5 TeV for the detected gamma rays.

The authors thank Scott Delay and Michael Schneider for their dedicated efforts on the Milagro experiment. We thank Stan Hunter for providing the EGRET data. This work has been supported by the National Science Foundation (under Grants No. PHY-0075326, No. PHY-0096256, No. PHY-0097315, No. PHY-0206656, No. PHY-0245143, No. PHY-0245234, No. PHY-0302000, and ATM-0002744) the U.S. Department of Energy (Office of High-Energy Physics), Los Alamos National Laboratory, the University of California, and the Institute of Geophysics and Planetary Physics.

*Present address: Department of Physics, University of UT, 115 South 1400 East, Salt Lake City, UT 84112.
†Present address: Max-Planck-Institut für Kernphysik, Postfach 103980, D-69029 Heidelberg, Germany.
‡Present address: NASA Goddard Space Flight Center, Greenbelt, MD 20771.
§Present address: MA Institute of Technology, Building 37-664H, 77 MA Avenue, Cambridge, MA 02139.

[1] R. C. Hartman *et al.*, Astrophys. J. **230**, 597 (1979).
[2] S. D. Hunter *et al.*, Astrophys. J. **481**, 205 (1997).
[3] C. D. Dermer, Astron. Astrophys. **162**, 223 (1986).
[4] P. Chardonnet *et al.*, Astrophys. J. **454**, 774 (1995).
[5] E. G. Berezhko and H. J. Völk, Astrophys. J. **540**, 923 (2000).
[6] F. A. Aharonian and A. M. Atoyan, astro-ph/0009009.
[7] A. Strong *et al.*, Astrophys. J. **613**, 962 (2004).
[8] S. LeBohec *et al.*, Astrophys. J. **539**, 209 (2000).
[9] F. Aharonian *et al.*, Astron. Astrophys. **375**, 1008 (2001).
[10] M. Amenomori *et al.*, Astrophys. J. **580**, 887 (2002).
[11] A. Borione *et al.*,Astrophys. J. **493**, 175 (1998).
[12] R. Atkins *et al.*, Nucl. Instrum. Methods Phys. Res., Sect. A **449**, 478 (2000).
[13] R. Atkins *et al.*, Astrophys. J. **595**, 803 (2003).
[14] The EGRET data were provided by S. D. Hunter (private communication).
[15] D. E. Alexandreas *et al.*, Nucl. Instrum. Methods Phys. Res., Sect. A **328**, 570 (1993).
[16] R. Fleysher *et al.*, Astrophys. J. **603**, 355 (2004).
[17] Calculated according to the statistic U', Eq. (8) of [16], a variant of the Li and Ma statistic [18] shown to converge to it in [16].
[18] T. Li and Y. Ma, Astrophys. J. **272**, 317 (1983).
[19] The slightly large $|b| < 7°$ band also excludes the possible influence of the Crab Nebula, known to emit gamma rays in the TeV energy region [13,20]. Disks of radius 5° centered on the Sun and Moon, two moving sinks of comic rays, were also excluded.
[20] T. C. Weekes *et al.*, Astrophys. J. **342**, 379 (1989).
[21] R. Atkins *et al.* (to be published).
[22] D. L. Hall *et al.*, J. Geophys. Res. **104**, 6749 (1999).
[23] K. Munakata *et al.*, Phys. Rev. D **56**, 23 (1997).
[24] M. Amenomori *et al.*, Phys. Rev. Lett. **93**, 061101 (2004).
[25] The fractional excess can be split after the fact as $\mathcal{F} = (8.30 \pm 1.58) \times 10^{-4}$ and $\mathcal{F} = (3.22 \pm 1.06) \times 10^{-4}$ inside and outside the cygnus region of R1, respectively. A Milagro investigation of the morphology and spectral behavior of the cygnus-vicinity signals is in progress, with a larger statistical sample and different methodologies.
[26] T. M. Dame *et al.*, Astrophys. J. **547**, 792 (2001).
[27] Multiwavelength Milky Way maps are shown in http://adc.gsfc.nasa.gov/mw/mmw_images.html#maps.

[28] For more recent data, event energy reconstruction is made feasible by locating the shower core with an ''outrigger'' array installed around the pond detector.
[29] η varies by $\pm 10\%$ for α_γ between 2.5 and 2.9.
[30] K. Asakimori *et al.*, Astrophys. J. **502**, 278 (1998).The error on this flux is negligible compared to 30%. The contribution from nuclei heavier than H and He is negligible.
[31] M. Pohl and J. A. Esposito, Astrophys. J. **507**, 327 (1998).